J Solid State Electrochem (2001) 5: 328–333
DOI 10.1007/s100080000139

ORIGINAL PAPER

Takashi Itoh · Koji Abe · Mohamed Mohamedi
Matsuhiko Nishizawa · Isamu Uchida

In situ SERS spectroscopy of Ag-modified pyrolytic graphite in organic electrolytes

Received: 4 February 2000 / Accepted: 7 April 2000 / Published online: 9 May 2001

Abstract Surface enhanced Raman scattering (SERS) has been applied to study the lithium intercalation/deintercalation process at the interface of a pyrolytic graphite electrode with propylene and ethylene carbonate containing organic solutions. We have focused on the lattice vibration of the most outer graphite surface layer simultaneously with cyclic voltammetric measurements. In situ Raman spectroscopy performed in this way allowed us to determine the *La* value that describes the size of graphitic microcrystallites along the *a*-axis. It was found that the *La* value decreases when the electrode is polarized to potentials between 0.02 and 1.0 V. This phenomenon can be correlated with the intercalation of lithium ions into the graphene structure. According to the spectral change, the size of the graphitic microcrystallites shows reversible behavior with potential cycling at the surface of the electrode.

Keywords Raman spectroscopy · Surface enhanced Raman scattering · Graphite electrodes · Lithium ion secondary batteries · Electrochemical intercalation

Introduction

When coupled with electrochemical techniques, in situ Raman spectroscopy is a powerful tool for investigating electrochemical processes [1, 2]. This combination has proven to be very advantageous in studying reactions occurring at the interface of organic electrolytes with the electrode materials employed in lithium ion batteries, such as $LiCoO_2$ [3], highly oriented pyrolytic graphite (HOPG) [4], mesocarbon microbeads [5] and lithium metal surfaces [6]. Because only the near-surface characteristics of the carbon materials affect the battery performance, interfacial and near-surface information, including electronic states, is necessary to understand the parameters controlling the cell performance. Recently, Besenhard et al. [7] have proposed a surface intercalation/deintercalation model of the HOPG electrode, which describes the intercalation/deintercalation of lithium in organic solutions by correlating electrochemical measurements and expansion recordings. They report that the HOPG surface expands in the direction of the *c*-axis during the intercalation of lithium. It is desirable to compare this with the evidence of other measurement methods, for example spectroscopic techniques. However, it is very difficult to obtain comprehensive information about the lithiation phenomenon when solely spectroscopic measurements are used. Therefore we aim to use a combination of electrochemical and spectroscopic measurements simultaneously to analyze the lithiation process.

Since 1974, the surface enhanced Raman scattering (SERS) effect has been extensively exploited to study the microscopic features of adsorbed molecules on SERS-active materials [1, 2, 8, 9, 10, 11, 12]. When SERS is applied, the Raman intensity of adsorbed molecules at the electrode surface is enhanced by a factor of 10^5–10^6 when compared with that for free molecules [2]. Recent in situ SERS studies aimed at the elucidation of electrochemical reactions were mainly concerned with the lattice damage of a glassy carbon (GC) electrode coated with Ag [9], and adsorption of water [10] or organic molecules [11] on Ag electrodes in aqueous solutions. Ishida et al. [12] investigated carbon materials covered with silver and observed that the Raman intensity related to carbon in such a specimen was enhanced, compared with the bare material. Whereas non-SERS Raman spectroscopy yields information about a thin layer of ca. 40 nm thickness, they reportedly were able to observe lattice vibration from the outermost surface of SERS-inactive materials [9, 12]. A combination of this technique and electrochemical methods (cyclic voltammetry,

T. Itoh · K. Abe · M. Mohamedi · M. Nishizawa · I. Uchida (✉)
Department of Applied Chemistry,
Graduate School of Engineering, Tohoku University,
Aramaki-Aoba, Aoba-ku, Sendai 980-8579, Japan
E-mail: uchida@est.che.tohoku.ac.jp
Tel.: +81-22-2177220
Fax: +81-22-2148646

CV) in situ should be able to give a definitive picture of the dynamics of the electrode reaction in the interfacial region between electrode and electrolyte, which is the region that determines battery performance.

In this paper, we report an in situ SERS study of graphite surfaces at the interface of pyrolytic graphite covered with a thin layer of Ag (Ag-modified PG electrode), with propylene and ethylene carbonate containing organic solutions. We used a Raman spectroscopic system with a multi-channel optical detector, which enabled us to record a spectrum of ca. 1400 cm^{-1} width in a few seconds. The Raman spectra and CV were measured simultaneously during continuous scanning of the electrode potential.

Experimental

A special cell was designed and constructed for the simultaneous use of in situ Raman and CV measurements. This is illustrated in Fig. 1. An air-tight cell made of Pyrex glass was equipped with a sapphire window for optical measurements. The cell was assembled in an argon-filled dry box (Miwa, MDB-1B + MS-P15S).

A 3×3×3 mm^3 working electrode (WE) was made of pyrolytic graphite (Union Carbide). The effective area of the electrode in contact with the electrolyte was 9 mm^2. A thermal shrinking tube (Pennitto) was used to provide non-leakage shielding of the graphite with a Pyrex electrode holder. Two types of electrodes were employed in this work, one exposing the basal plane and the other exposing the edge planes of the PG. These electrodes were made by appropriate assembly cutting, and subsequently by polishing one end of the tube. The electrode prepared in this way was cleaned ultrasonically in distilled water and dried in a high-vacuum oven. The electrode was subsequently evacuated and Ag was vacuum-deposited on the PG substrates (edge and basal planes) under a vacuum of 1.0×10^{-5} Torr. The thickness of the Ag layer on the PG was several tens of nanometers. The surface morphology of the coating was examined with a scanning electron microscopy (SEM, Hitachi H-8100). The reference (RE) and counter electrodes (CE) were lithium foils pressed on nickel meshes. All potentials reported in this work were measured against the Li/Li^+ (1 M $LiClO_4$) reference electrode. The electrolyte was a mixture of propylene carbonate (PC) and ethylene carbonate (EC) containing 1 M $LiClO_4$ (Mitsubishi Chemical, battery grade).

The electrochemical measurements were performed with a Solartron 1267 potentiostat coupled with Corrware (Scribner Associates). In CV experiments, the potential of the working electrode was swept between the open circuit potential (2.8 V) and 0.02 V with a scan rate of 0.2 mV/s.

The radiation (514.5 nm, 40 mW) of an argon ion laser (Coherent, Innova 70) was focused on a 0.1 mm×1.0 mm spot on the electrode surface at an incident angle of ca. 60°. The laser power density was 40 W/cm^2. The scattered light was collected and efficiently converged at the entrance slit of a triple stage spectrograph (Jasco, TRS-300). The effective spectral width of the entrance slit was approximately 48 cm^{-1}. In situ measurements of Raman spectra were performed with a diode array detector (Hamamatsu Photonics, M2493) equipped with an intensifier (Hamamatsu Photonics, M2492). The Raman system described above enabled us to obtain a spectrum from 600 cm^{-1} to 2000 cm^{-1} in 512 data points of the diode array.

The Raman spectra and CV were measured simultaneously. Raman spectra were recorded periodically while the electrode potential was swept at intervals of 100 mV. The accumulation time of the Raman data was 75 s for each spectrum. Dark currents of the detector were determined and subtracted from the data, and the wavelength dependence of the measurement system was calibrated using the standard pattern of a tungsten lamp. All the experiments were carried out at room temperature.

Raman lines for Ag-modified PG electrodes were also analyzed by computer fitting (Origin, Microcal Software). The observed Raman spectra were first corrected by subtracting background spectra to determine the baseline. Next, two Lorentz functions, one for the frequency region between 1300 cm^{-1} and 1400 cm^{-1} and the other for the range between 1550 cm^{-1} and 1600 cm^{-1}, were used to fit the baseline-corrected Raman spectra. The Lorentz components give the integrated scattering intensity, the peak frequency and full width at half maximum.

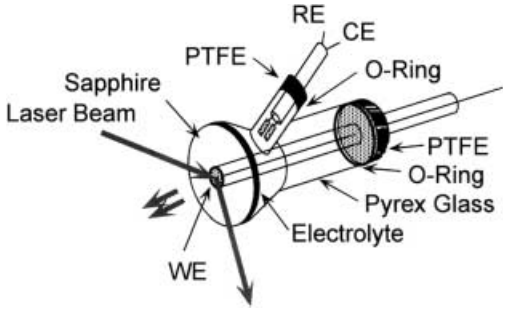

Fig. 1 Electrochemical cell for in situ Raman measurements

Results

Figure 2 shows SEM images of (a) basal and (b) edge planes of Ag-modified PG electrodes. The layered structure of graphite can be seen at some parts of the electrode in Fig. 2a. In Fig. 2b, one may observe the Ag spheroids on PG. The spheroid diameter is several hundred nanometers, which is in good agreement with the dimensions given elsewhere [12, 13].

In Fig. 3, SERS spectra of (a) the basal plane and (b) the edge plane of bare PG, and (c) the basal plane and (d) the edge plane of Ag-modified PG are shown. The following characteristics of these spectra were observed: (1) single lines at 1580 cm^{-1} in Fig. 3a and b can be assigned to the E_{2g} mode of the graphite structure [14]; (2) the Raman lines observed at 1350 cm^{-1} in Fig. 3c

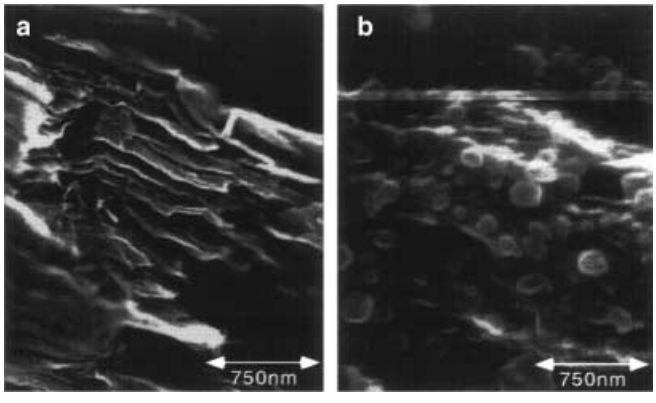

Fig. 2 SEM images of **a** the basal plane and **b** the edge plane of Ag-modified PG

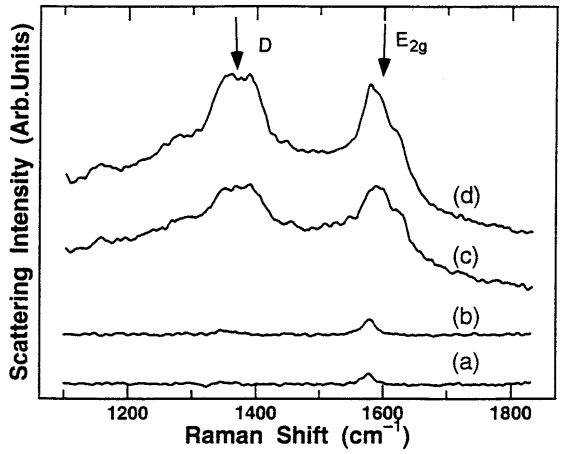

Fig. 3 Ex situ Raman spectra of *a* the basal plane and *b* the edge plane of bare PG, *c* the basal plane and *d* the edge plane of Ag-modified PG

and d are identical with the frequencies of the D band of graphitic structures [14].

The steady cycling CV curve recorded at a scan rate of 0.2 mV/s for the edge plane of the Ag-modified PG electrode immersed in PC + EC containing $LiClO_4$ is shown in Fig. 4. At first, the electrode was polarized with decreasing potential starting from the rest potential (2.8 V), and transient electrochemical responses were observed below 1.0 V. This reduction current can be attributed to the intercalation of lithium into the Ag-modified PG electrode [15]. When the potential scan is reversed at 0.02 V, an oxidation current is observed in the potential range from 0.02 V to 1.2 V, owing to the deintercalation of lithium ions from the Ag-modified PG electrode. In the case of the basal plane, we obtained almost the same shape of CV curve as that presented in Fig. 4.

Figure 5 shows the evolution of SERS spectra in the frequency range between 400 and 2200 cm^{-1} during the second cycle of the CV with (a) decreasing and (b) increasing potential. As can be seen, apart from the Raman lines characteristic for the D band and the E_{2g} mode of graphite (marked with arrows in the figure), others assigned to the organic solution were observed [4, 5, 16]. The frequencies of the E_{2g} and D bands in Fig. 5a and b are almost the same as those of Fig. 3b.

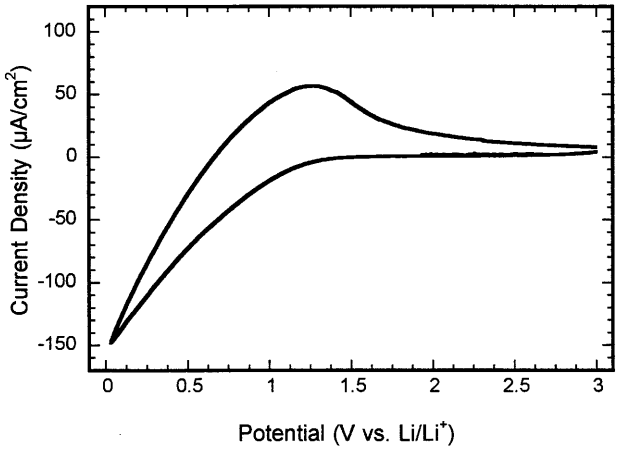

Fig. 4 Cyclic voltammograms of Ag-modified PG (edge plane) electrodes in PC + EC containing 1 M $LiClO_4$. Scan rate is 0.2 mV/s

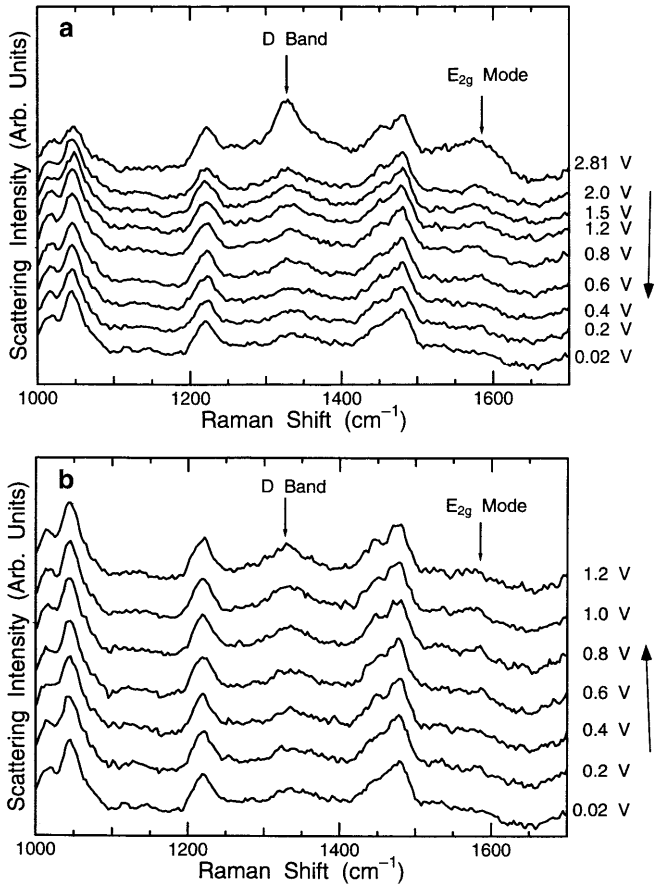

Fig. 5 Variation of in situ Raman spectra with **a** decreasing and **b** increasing potential applied to the Ag-modified PG (edge plane) electrodes in PC + EC containing 1 M $LiClO_4$. Scan rate is 0.2 mV/s

Since the Raman shift for the Ag-modified PG electrodes clearly showed potential dependence, we tried to determine more precisely the potential dependence as well as other parameters of the lines, assuming Lorentzian curves to be fitted to each Raman lines. The Lorentz fitting gives the peak position, the full width at half maximum and the peak height. The scattering intensity is provided by the integration of the Lorentzian. The effects of the electrode potential recorded during the second and third scans of CV on (a) Raman shift, (b) full width at half maximum (FWHM) and (c) scattering intensity of the Raman lines of the D band and E_{2g} mode are shown in Figs. 6 and 7, respectively.

The Raman frequency of the D band was 1325 cm^{-1} at 2.8 V and appeared to be almost independent of the electrode potentials in the range 2.8–1.0 V. The D band frequency of Ag-modified PG electrodes was lower in comparison with that for bare PG. When the potential was decreased from 1.0 to 0.02 V, the Raman frequency

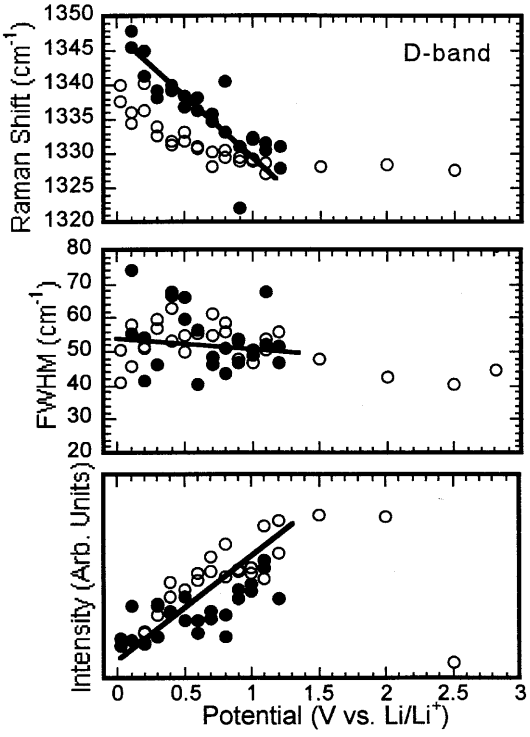

Fig. 6 D band for the Ag-modified PG (edge plane) electrodes: effect of the electrode potential on (*top*) Raman shift, (*middle*) full width at half maximum (FWHM) and (*bottom*) scattering intensity of the Raman lines. *Open markers*: decreasing potential; *solid markers*: increasing potential

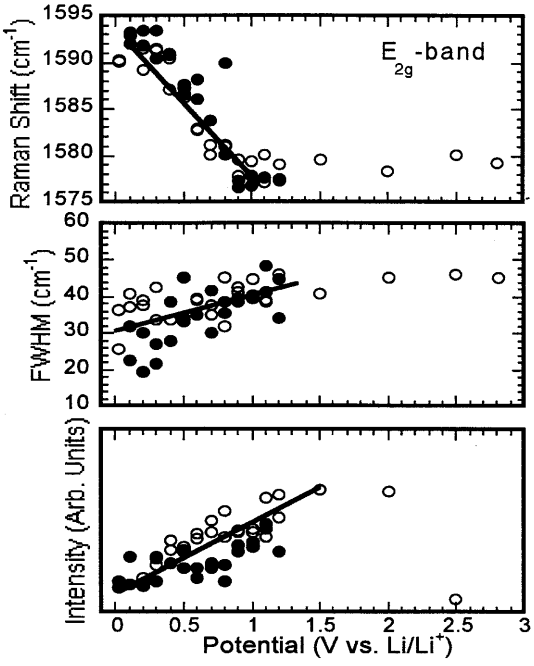

Fig. 7 E_{2g} band for the Ag-modified PG (edge plane) electrodes: effect of the electrode potential on (*top*) Raman shift, (*middle*) full width at half maximum (FWHM) and (*bottom*) scattering intensity of the Raman lines. *Open markers*: decreasing potential; *solid markers*: increasing potential

of the D band shifted up to 1342 cm^{-1} and the scattering intensity decreased.

The Raman frequency of the E_{2g} mode was equal to ca. 1580 cm^{-1}, being almost constant in the potential range between 2.8 and 1.0 V. When the potential was decreased from 1.0 to 0.02 V, the Raman frequency of E_{2g} shifted up to 1592 cm^{-1} and the scattering intensity of E_{2g} decreased. The FWHM of the E_{2g} mode showed almost no potential dependence.

Discussion

The difference in Raman and SERS spectra of PG is most clearly illustrated by Fig. 3. This shows especially a large difference in the Raman intensities of the D band. Since the D band of graphite is related to the disordered structure of the graphene layer [9, 12], one may infer from Fig. 3 that Ag particles are selectively located on those sites of the graphite surface that have a disordered structure. Therefore the Raman intensity of the D band is enhanced, as has been suggested by others [9, 12].

Figure 6a and b show that the characteristics of the D band of the Ag-modified PG electrode depend on the potential during the intercalation/deintercalation of lithium. In the potential range between 0.02 and 1.0 V, its frequency shifts reversibly upwards with decreasing and increasing potentials. On the other hand, the PG electrode without Ag did not show such a potential dependence. From this behavior we can obtain information about the vibration dynamics of the outermost layer of the electrode surface. Since the frequency shift of the D band is related to the actual state of the electrode surface, the vibrational frequency should be affected by the mass of Ag atoms on the Ag-modified PG electrode surface. Generally, the Raman frequency is related to the force constant and effective mass [17], and the shift of the D band observed in Fig. 3 can be attributed to an increase of the effective mass due to the coating of Ag on the PG electrode surface.

As shown in Fig. 6, the Raman intensity of the D band decreased at potentials below 1.0 V with decreasing potential. At these potentials the conductivity becomes higher with progressive lithium insertion [18]. The conductivity of the electrode increases while the Raman intensity decreases. This result may be attributed to a reduction in optical skin depth [3].

This can be seen in the relationship between optical skin depth (δ) and the electrical conductivity (σ) [3]:

$$\delta = \frac{2}{\sqrt{\mu\sigma\omega}} \tag{1}$$

where μ and ω are the magnetic permeability and the angular frequency of the electromagnetic field, respectively. If μ and ω are constant, then δ, which also is the penetration depth of the Raman measurement from the electrode surface (i.e. the information of Raman scattering intensity), decreases with increasing σ; therefore if

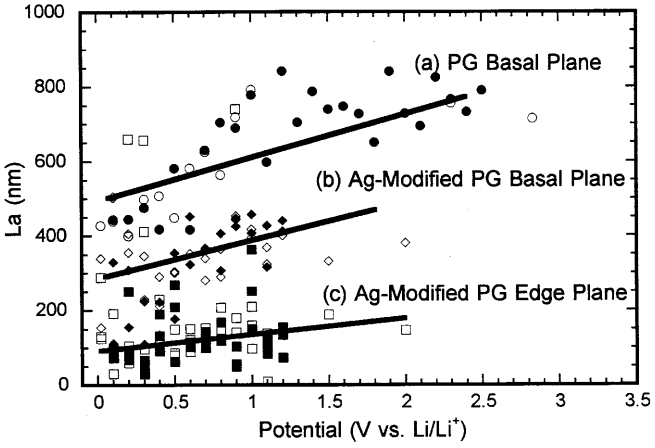

Fig. 8 Potential dependence of the *La* value for *a* PG (basal plane) (○, ●), *b* PG (basal plane) (◇, ◆) and (*c*) Ag-modified PG (edge plane) (□, ■) electrodes in PC + EC containing 1 M $LiClO_4$. *Open markers*: decreasing potential; *solid markers*: increasing potential

the conductivity of the electrode is increased, the observed Raman intensity will be decreased.

The next issue is the effect of potential on the E_{2g} mode for the Ag-modified PG electrodes in Fig. 7. The Raman frequency of the E_{2g} mode exhibited a remarkable potential dependence, shifting up with decreasing potential, and vice versa. Dresselhaus and Dresselhaus [19] have described the relationship between the lithium content of graphite and the frequency of the E_2 mode. In their paper, the Raman frequency of the E_{2g} mode shifts down on increasing the content of lithium metal in graphite. This is attributed to the effect of a graphite intercalation compound (GIC). In the case of an acceptor-type GIC (i.e. halogen), the frequency is up-shifted with increasing halogen content. According to Besenhard et al. [7], lithium ions are solvated in organic solutions and their desolvation occurs at the surface when lithium ions intercalate into graphite. Therefore, when looking at the outermost surface layer of graphite in organic solutions by Raman spectroscopy, we have to distinguish it from the inner phase. The observed up-shift of frequency in the potential range between 1.0 V and 0.02 V would be in agreement with both the donor/acceptor-type GIC behavior according to Dresselhaus and Dresselhaus [19], and the desolvation upon intercalation according to Besenhard et al. [7].

It is known that the ratio of the intensity of the D band to the intensity of the E_{2g} band is related to the size of graphitic microcrystallites along the *a*-axis [20], i.e. the average length of the lattice, *La*. The dependence of the *La* values on the potential is presented in Fig. 8, where (a), (b) and (c) correspond to the basal plane, Ag-modified PG basal plane and Ag-modified PG edge plane, respectively. Within the potential range from the rest potential (2.8 V) to around 1.2 V, the *La* values do not show any clear dependence on the potential. In the case of the basal plane or Ag-modified PG basal plane, *La* values were distinctly larger than those for the edge plane. However, below 1.2 V, that is, just after the intercalation of lithium ions starts to take place, the *La* values decreased. Apparently, this dependence of *La* on potential is reversible.

Dahn [21] investigated the graphite electrode during the intercalation/deintercalation of lithium by the use of the in situ XRD technique, reporting that the lattice constant along the *c*-axis in the unit cell of graphite increases during the intercalation and decreases during the deintercalation. Taking this into account, we suppose that the E_{2g} mode of the in-plane vibration may change owing to increased interaction along the *c*-axis. Therefore, the lattice is stressed along the in-plane direction, which affects the two Raman bands. As a result, the *La* value of the Ag-modified PG electrodes decreases when the electrode potential is decreasing. The same consideration would apply in the case of PG. Further studies are required to explore the correlation between the value of *La*, the extent of intercalation/deintercalation of lithium, and the tendency to distortion or destruction of the graphite surface [22].

Conclusions

A SERS investigation of the interface between Ag-modified PG electrodes and organic solutions was carried out by in situ Raman and CV measurements. The intensities of the D band and E_{2g} mode for the Ag-modified PG electrodes are distinctly higher than those for the bare PG electrodes. The intensity of the Raman line of the E_{2g} mode was observed to vary reversibly with the electrode potential. The Raman shift of this line was also reversibly potential dependent and could be related to the intercalation/deintercalation phenomenon of solvated lithium ions.

The *La* value, which is related to the size of graphitic microcrystallites along the *a*-axis, was determined from the relative Raman intensities of the D and E_{2g} bands as a function of the potential. The effect of potential on the *La* value can be clearly correlated with the structural changes taking place due to intercalation/deintercalation of lithium, and appear to be reversible.

Acknowledgements The present work was partly supported by Grants-in-Aid for Priority Area A (No. 10148205, 10131211 and 11118213 for "Electrochemistry of Ordered Interfaces" and No. 12022208 for "New Protium Function") and Encouragement of Young Scientists (No. 12750724), from the Ministry of Education, Science, Sports and Culture, Japan.

References

1. Gale RJ (1988) Spectroelectrochemistry, Plenum Press, New York
2. Chang RK, Furtak TE (eds) (1982) Surface enhanced Raman scattering. Plenum Press, New York
3. Itoh T, Sato H, Nishina T, Matsue T, Uchida I (1997) J Power Sources 68:333

4. Inaba M, Yoshida H, Ogumi Z, Abe T, Mizutani Y, Asano M (1995) J Electrochem Soc 142:20
5. Inaba M, Yoshida H, Ogumi Z (1996) J Electrochem Soc 143:2572
6. Itoh T, Matsutani Y, Uchida I (1996) Denki Kagaku 64:76
7. Besenhard JO, Winter M, Yang J, Biberacher W (1995) J Power Sources 54:228
8. Fleischman M, Hendra PJ, McQuillan AJ (1974) Chem Phys Lett 26:163
9. Alsmayer YW, McCreery RL (1991) Anal Chem 63:1289
10. Itoh T, Sasaki Y, Maeda T, Horie C (1997) Surf Sci 389:333
11. Tian ZQ, Sigalaev SK, Zou SZ, Mao BW, Funtikov AM, Kazarionov VE (1994) Electrochim Acta 39:2195
12. Ishida H, Hukuda H, Katagiri G, Ishitani A (1986) Appl Spectrosc 40:322
13. Sebbett RS, Scott GD (1950) J Opt Soc Am 40:203
14. Holzwarth NAW, Rabii S, Girifalco LA (1978) Phys Rev B 18:5190
15. Levi MD, Aubach D (1997) J Electroanal Chem 421:79
16. Inaba M, Yoshida H, Ogumi Z (1996) J Electrochem Soc 143:2572
17. Colthup NB, Daly LH, Wiberley SE (1990) Introduction to infrared and Raman spectroscopy. Academic Press, San Diego
18. Nishizawa M, Koshika H, Hashitani R, Itoh T, Abe T, Uchida I (1999) J Phys Chem B 103:4933
19. Dresselhaus MS, Dresselhaus G (1981) Adv Phys 30:139
20. Kinoshita K (1987) Carbon – electrochemical and physicochemical properties. Wiley, New York
21. Dahn JR (1991) Phys Rev B 44:44
22. Inaba M, Siroma Z, Funabiki A, Ogumi Z (1996) Langmuir 12:1535